



# Bioinspired Synthesis of ZnO@polydopamine/Au for Label-Free Photoelectrochemical Immunoassay of Amyloid- $\beta$ Protein

Guangli He<sup>1</sup>, Yue Zhou<sup>1</sup>, Mifang Li<sup>2</sup>, Yanzhen Guo<sup>1</sup>, Hang Yin<sup>1</sup>, Baocheng Yang<sup>1\*</sup>, Shouren Zhang<sup>1\*</sup> and Yibiao Liu<sup>2\*</sup>

<sup>1</sup>Henan Key Laboratory of Nanocomposites and Applications, Institute of Nanostructured Functional Materials, Huanghe Science and Technology College, Zhengzhou, China, <sup>2</sup>Shenzhen Longgang Central Hospital (The Second Affiliated Hospital of the Chinese University of Hong Kong, Shenzhen, China

## OPEN ACCESS

### Edited by:

Tailin Xu,  
Shenzhen University, China

### Reviewed by:

Shuqi Wang,  
Suzhou Institute of Nano-tech and  
Nano-bionics (CAS), China  
Guangyao Zhang,  
Qingdao University, China

### \*Correspondence:

Baocheng Yang  
baochengyang@infm.hhstu.edu.cn  
Shouren Zhang  
shourenzhang@infm.hhstu.edu.cn  
Yibiao Liu  
liyubiao12345@126.com

### Specialty section:

This article was submitted to  
Biosensors and Biomolecular  
Electronics,  
a section of the journal  
Frontiers in Bioengineering and  
Biotechnology

**Received:** 15 September 2021

**Accepted:** 18 October 2021

**Published:** 16 November 2021

### Citation:

He G, Zhou Y, Li M, Guo Y, Yin H,  
Yang B, Zhang S and Liu Y (2021)  
Bioinspired Synthesis of ZnO@  
polydopamine/Au for Label-Free  
Photoelectrochemical Immunoassay  
of Amyloid- $\beta$  Protein.  
Front. Bioeng. Biotechnol. 9:777344.  
doi: 10.3389/fbioe.2021.777344

Amyloid- $\beta$  protein (A $\beta$ ) is an important biomarker and plays a key role in the early stage of Alzheimer's disease (AD). Here, an ultrasensitive photoelectrochemical (PEC) sensor based on ZnO@polydopamine/Au nanocomposites was constructed for quantitative detection of A $\beta$ . In this sensing system, the ZnO nanorod array decorated with PDA films and gold nanoparticles (Au NPs) have excellent visible-light activity. The PDA film was used as a sensitizer for charge separation, and it also was used for antibody binding. Moreover, Au NPs were loaded on the surface of PDA film by *in situ* deposition, which further improved the charge transfer efficiency and the PEC activity in visible light due to the localized surface plasmon resonance effect of Au NPs. Therefore, in ZnO@polydopamine/Au nanocomposites, a significantly enhanced photocurrent response was obtained on this photoelectrode, which provides a good and reliable signal for early detection of AD. Under the optimized conditions, the PEC immunosensor displayed a wide linear range from 1 pg/mL to 100 ng/mL and a low detection limit of 0.26 pg/mL. In addition, this PEC immunosensor also presented good selectivity, stability, and reproducibility. This work may provide a promising point-of-care testing method toward advanced PEC immunoassays for AD biomarkers.

**Keywords:** photoelectrochemical sensor, ZnO, polydopamine, gold nanoparticles, Alzheimer's disease

## INTRODUCTION

As a most prevalent type of dementia, Alzheimer's disease (AD) is a fatal and irreversible neurodegenerative disorder, occurring mainly in aged people.(Evans, Funkenstein et al., 1989; Matthews, Arthur et al., 2013) Although massive effort has been made to cure this disease, there is still no efficient treatment for it. AD is marked by a slow degeneration progression and the neurodegeneration process starts several decades before the first clinical symptoms appear.(Jack et al., 2010; Selkoe 2012; Yang et al., 2021) Therefore, early diagnosis of AD allows timely treatment to ameliorate the deterioration symptoms of the patient, which has important directive significance to clinical works.(Butterfield, Drake et al., 2002; Hardy 2002; Jack et al., 2010; Murphy and Rd 2010) One of the important traits of AD is cerebral extracellular amyloid plaques, which are formed through aggregation of amyloid- $\beta$  (A $\beta$ ) protein. A $\beta$  protein is a polypeptide consisting of 39–42 amino acids. There are two primary variants: A $\beta$ 40 and A $\beta$ 42. PET

and the level of A $\beta$  (A $\beta$ 40, A $\beta$ 42) in cerebrospinal fluid (CSF) are the gold standard of AD clinical diagnosis. (Grimmer, Riemenschneider et al., 2009; Marcus, Mena et al., 2014; Guilherme, Marina et al., 2020) However, this diagnosis method is unlikely to become popularized in the public because of high-cost PET and unavailable CSF. Therefore, the development of low-cost, noninvasive, and accessible tools to accurately quantify A $\beta$  protein in blood for the early diagnosis of AD is required. (Nakamura, Kaneko et al., 2018; Laís Canniatti, Isabella et al., 2019) In blood, the physiological concentrations of A $\beta$  is several picograms per milliliter. To date, a great deal of sensing techniques has been performed to detect A $\beta$  protein, including ELISA (Linan, Son et al., 2016), ion mobility-mass spectrometry (IM-MS) (Obata, Murakami et al., 2020), colorimetric biosensor (Xi, Shuangling et al., 2021), electrochemical (Carneiro, Loureiro et al., 2017), fluorescence (Lee, Park et al., 2019; Wang, Du et al., 2020; Wen-Kai, Liu et al., 2021), surface-enhanced Raman spectroscopy (Yang, Hwang et al., 2019), and photoelectrochemical (PEC) immunosensors (Wang, Fan et al., 2018). Among them, the PEC biosensor is an innovative and attractive analytical technique for quantitative study in the biological analysis due to its intrinsic merits such as label-free, high signal-to-noise ratio, rapid response, and is more readily miniaturized. (Shu and Tang 2019)

For the construction of the PEC biosensor, various kinds of semiconductor materials have been developed to construct the photoelectrode for PEC sensing. Zinc oxide (ZnO) is one of the most extensively used n-type semiconductor photoactive substrates with the advantages of environmental friendliness, abundant natural resources, low cost, and high stability. (Wei, Ke et al., 2012; Zhang, Wang et al., 2016) However, ZnO has the inherent limitations of inefficient utilization of sunlight and low separation efficiency of electron hole, which cannot meet the demands for higher sensitivity of PEC detection. To improve the light-harvesting efficiency and prolong the life of photo-generated carriers, combining with plasmon metals including Au, Ag, and Cu exhibits great superiority in improving the light absorption range and separation efficiency of charge carriers of ZnO-based systems over the other strategies due to the surface plasmon resonance (SPR) effect. (Zheng, Zheng et al., 2007; Xiao, Liu et al., 2015; Kang, Yan et al., 2016; Yang, Li et al., 2017; Zhang, He et al., 2018) Based on the localized surface plasmon resonance (LSPR) of Au nanoparticles (Au NPs), the strong visible light absorption and the effective photo-generated carrier separation at the metal-semiconductor interface can successfully generate remarkable readout photocurrent signals. (Zhu, Zhang et al., 2016; Zhang, Wang et al., 2018; Dong, Xu et al., 2019) For PEC biosensor, the efficient immobilization of biomolecules on photoactive materials of the photoelectrode is also a crucial factor for achieving excellent performance. (Shu and Tang 2019) For ZnO/Au substrates, the antibody immobilization is mainly through Au-NH<sub>2</sub> bonding (Parviz Norouzi and Ganjali 2011; Gasparotto, Costa et al., 2017), but the amount of the immobilized antibody is limited by the low

Au content. Recently, inspired by the mussel-adhesion phenomenon, polydopamine (PDA) has attracted intensive attention as a multifunctional biocompatible material with unique properties. (Lee, Dellatore et al., 2007; Lyngge, van der Westen et al., 2011; Liu, Ai et al., 2014) Through self-polymerization of dopamine in alkaline aqueous solutions at room temperature, PDA can coat on the surface of various kinds of substrates with strong affinity. The as-formed adherent PDA thin film has abundant active functional groups (catechol, amine, indole, and quinone), capable to serve as universal platforms including cross-linker reagents for biomolecule immobilization and reductants for *in situ* metal deposition. Besides, PDA possesses broadband light absorption and can work as an electron donor. (Hu, He et al., 2014; Wang, Ma et al., 2017; Yu, Huang et al., 2018; He, Gao et al., 2019) Thus, PDA that is used to build up PEC immunosensor exhibits great advantages as a multifunctional platform.

In this work, a novel plasmonic PEC immunosensor was successfully constructed based on ZnO nanorod array@polydopamine heterointerface modified with Au NPs (ZnO@PDA/Au) for sensitive detection of A $\beta$ . The stepwise process for the PEC immunosensor fabrication and the charge transfer mechanism are displayed in **Figure 1**. The PDA coating involving in the system is used as a multifunctional platform such as a sensitizer for enhancing the photo-to-electron conversion efficiency, a binder for antibody bonding, and a reductant for *in situ* Au deposition. Both PDA film and Au NPs can enhance the light absorption and loading content of antibody. The as-prepared PEC immunosensor realized label-free detection of A $\beta$ , which exhibits a wide linear range from 1 pg/mL to 100 ng/mL, low detection limit of 0.26 pg/mL, high sensitivity, and good stability. This work provides a promising future for the early diagnosis of AD.

## EXPERIMENTAL SECTION

### Chemicals and Materials

A $\beta$ 40, A $\beta$ 42, and A $\beta$ 42 antibodies were purchased from Bio-Techne China Co., Ltd (Shanghai, China). Bovine serum albumin (BSA) was obtained from Kuer Chemical Technology (Beijing) Co., Ltd (Beijing, China). Zinc nitrate hexahydrate (Zn(NO<sub>3</sub>)<sub>2</sub>·6H<sub>2</sub>O), ammonia hydroxide (NH<sub>3</sub>·H<sub>2</sub>O), ethylenediamine, and potassium permanganate (KMnO<sub>4</sub>) were acquired from Sinopharm Chemical Reagent Co., Ltd (Shanghai, China). Dopamine, sodium chloride (NaCl), potassium chloride (KCl), Na<sub>2</sub>HPO<sub>4</sub>·12H<sub>2</sub>O, KH<sub>2</sub>PO<sub>4</sub>, and ascorbic acid (AA) were purchased from Aladdin Biochemical Technology Co., Ltd., (Shanghai, China). Indium-doped tin oxide (ITO) conducting glass (sheet resistance 8  $\Omega$ ) was acquired from Wuhan Jingde Solar Technology Co., Ltd., (China). All the chemical reagents were of analytical grade and used directly as received. All the solutions used in all experiments were prepared with ultrapure water (Milli-Q, 18.2 M $\Omega$ ).

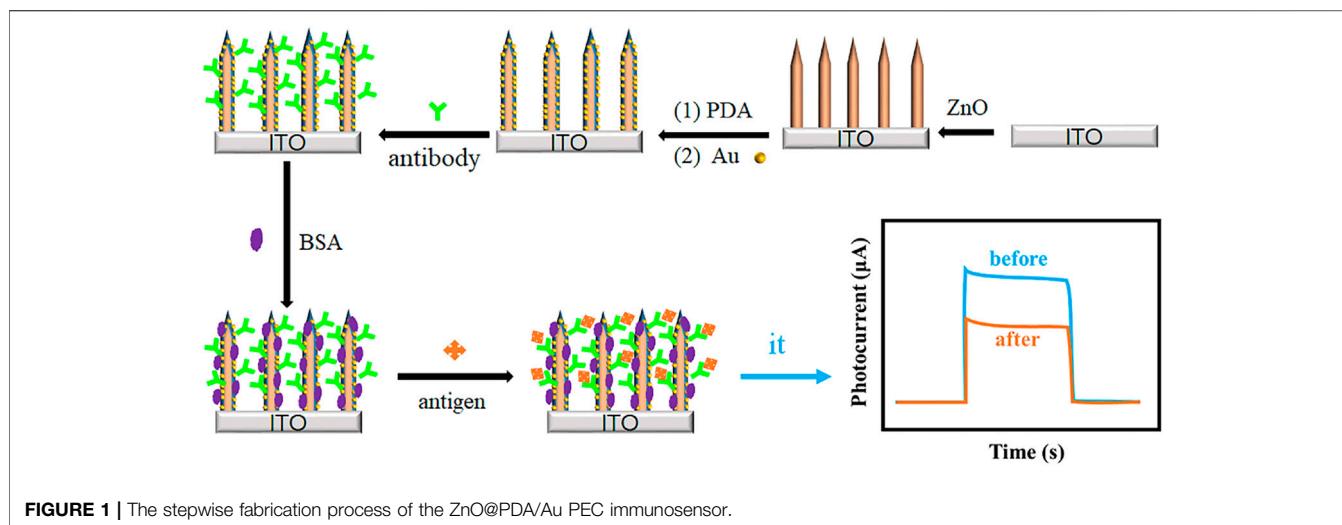


**FIGURE 1** | The stepwise fabrication process of the ZnO@PDA/Au PEC immunosensor.

## Characterization and Measurement

The morphology was characterized using field emission scanning electron microscopy (FESEM; Quanta 250, FEI, OR, United States). The energy-dispersive X-ray spectroscopy was used to reveal the elemental composition of all composites equipped with FESEM. The X-ray diffraction analyzer (XRD; Bruker D8 diffractometer, Germany) using Cu K $\alpha$  radiation (40 kV, 40 mA) was employed to determine the crystal phase of the obtained samples. The UV-vis diffuse reflectance spectra (DRS) of the samples were collected using a Thermo U-4100 UV-vis spectrophotometer. The X-ray photoelectron spectroscopy (XPS) data of the composite was obtained on a Thermo Scientific K-Alpha X-ray photoelectron spectrometer with a monochromatized MgK $\alpha$  X ray source. All the electrochemical measurements were carried out on a CHI760E Electrochemical Analyzer (Chenhua Instruments, Shanghai, China).

## Preparation of ZnO@PDA/Au Modified ITO Electrode

The ZnO nanorod array was grown onto ITO substrate based on the previous literature (Yang and Hu 2017; He, Gao et al., 2019). In brief, a piece of clean ITO (tailored as size of 2.5  $\times$  1 cm) was first immersed into freshly prepared KMnO $_4$  (5 mM) solution for 30 min at room temperature. After thoroughly rinsing with deionized water, the ITO was then placed with the conductive side facing down in a glass bottle with 10 mL precursor solution containing Zn(NO $_3$ ) $_2$  (0.1 M), ammonium hydroxide (3% v/v), and ethylenediamine (4% v/v). The reaction was carried out at 75°C in a water bath for 3 h. The obtained ZnO-ITO was rinsed with water and dried under gentle N $_2$  flow for later use. Then, the ZnO-ITO electrodes were further coated with PDA *via* a simple dip-coating method. Typically, the as-synthesized ZnO-ITO were dipped into 20 mL of Tris-HCl solution (10 mM, pH 8.5) containing 25 mg dopamine and kept for 4 h at room

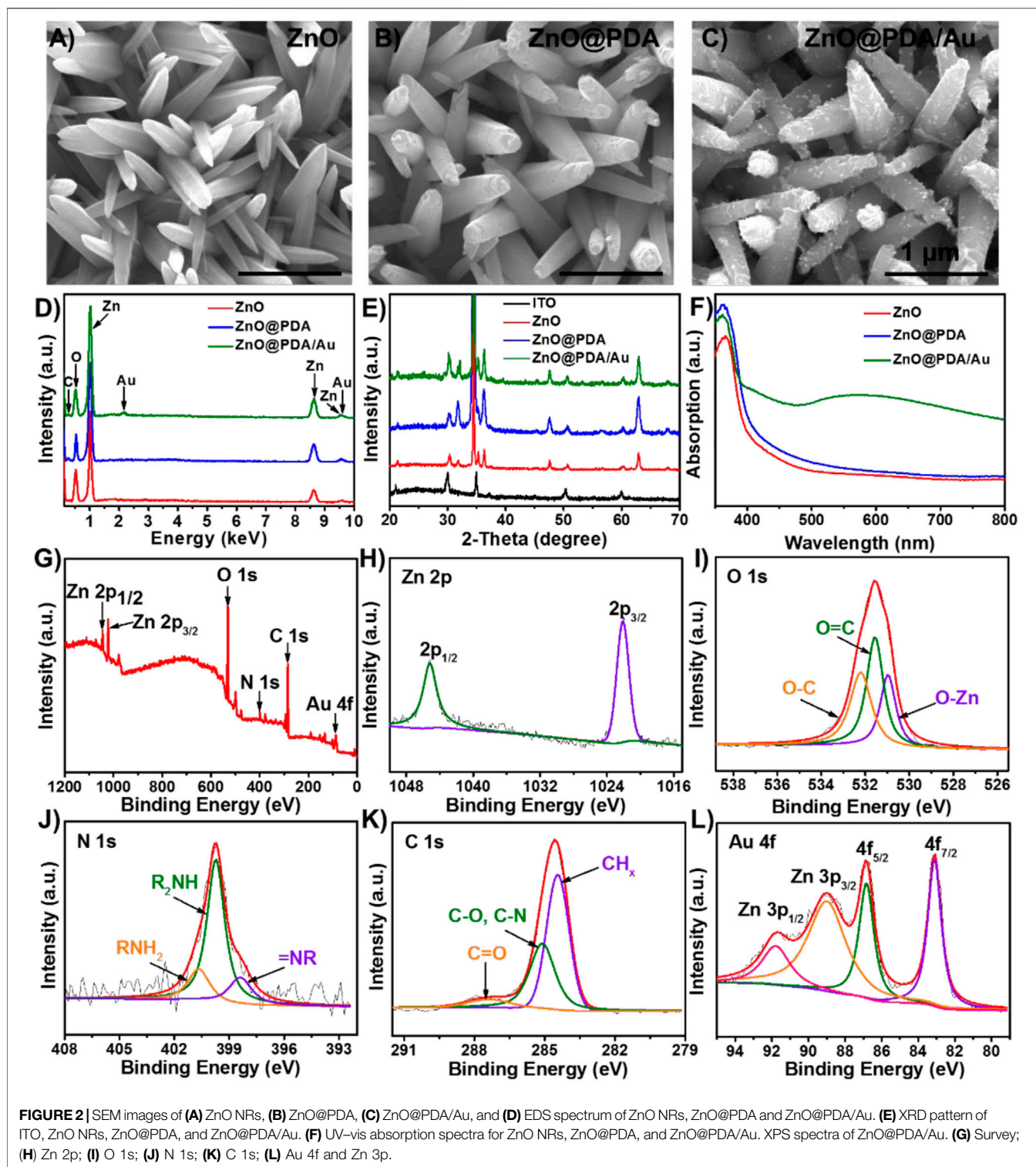
temperature, followed by gently rinsing with DI water several times. The as-obtained ZnO@PDA electrodes were stored at 4°C for the following use. Au NPs decorated ZnO@PDA-ITO was obtained based on the following *in situ* growth method. Then 0.2 mL of HAuCl $_4$  (1%) aqueous solution was added to 10 mL H $_2$ O solvent to obtain a homogeneous solution. Then the prepared ZnO@PDA-ITO were immersed into the solution and incubated for 60 min. These were then taken out and rinsed gently with DI water and stored at 4°C for next use.

## Construction of the Label-free PEC Immunosensors

First, the ZnO@PDA/Au electrode was incubated with 0.02 mL anti-A $\beta$  (10  $\mu$ g mL $^{-1}$ ) PBS solution (pH = 7.4) on the electrode surface for 1 h at room temperature. Second, the electrode was rinsed with PBS solution to remove the physical adsorption of antibodies. Third, the electrode was dipped into bovine serum albumin (BSA, 1 mg/mL) PBS solution for 1 h to block the non-specific binding sites. Finally, 10  $\mu$ L of A $\beta$  with different concentrations was dropped onto the electrode surface and incubated 1 h at room temperature. After thoroughly washing with PBS buffer, the sensors used for the following PEC detection were obtained.

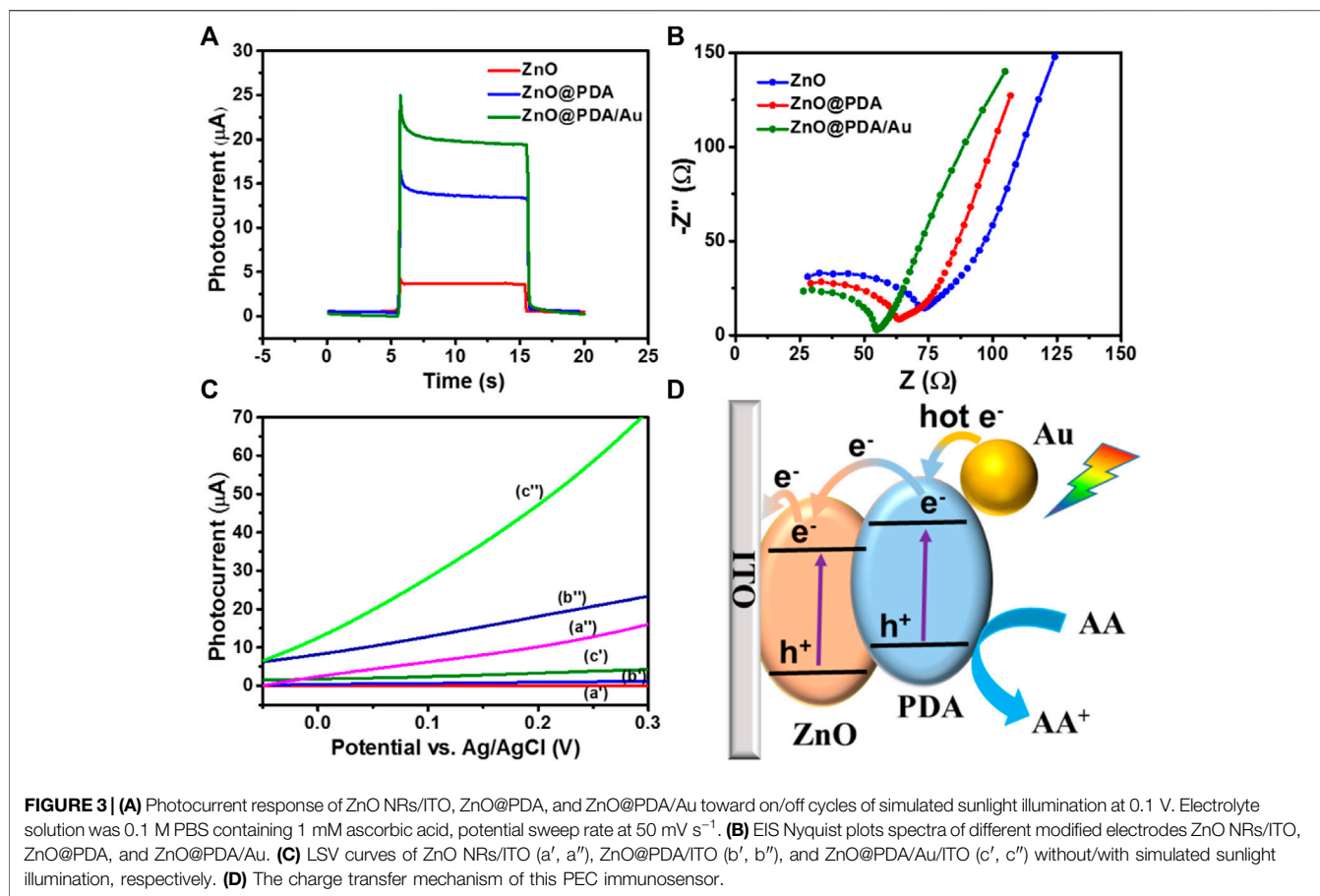
## Photoelectrochemical Detection

All the PEC tests were performed on a CHI 760E electrochemical workstation adopting a standard three-electrode system, in which the as-prepared photo-electrode was used as the working electrode, platinum (Pt) sheet as the counter electrode, and saturated Ag/AgCl electrode as the reference electrode. A 500-W Xe lamp equipped with an AM 1.5 G filter was employed as the irradiation source for the photo-response of the as-obtained photoelectrodes. The power density is 100 mW cm $^{-2}$ . 25 mL of PBS (0.1 M, pH 7.4) solution containing 1 mM AA served as the supporting



electrolyte. Linear sweep voltammetry (LSV) curves were recorded from  $-0.05$  to  $0.3$  V with a scan rate of  $50$   $\text{mV s}^{-1}$ . Electrochemical impedance spectroscopy (EIS) experiment was carried out at open circuit potential in the frequency

range of  $100$  kHz to  $0.1$  Hz with an amplitude of  $5$  mV. The photocurrent response measurements of the working electrode were collected under light irradiation switching on and off every  $10$  s at the applied potential of  $0.05$  V.



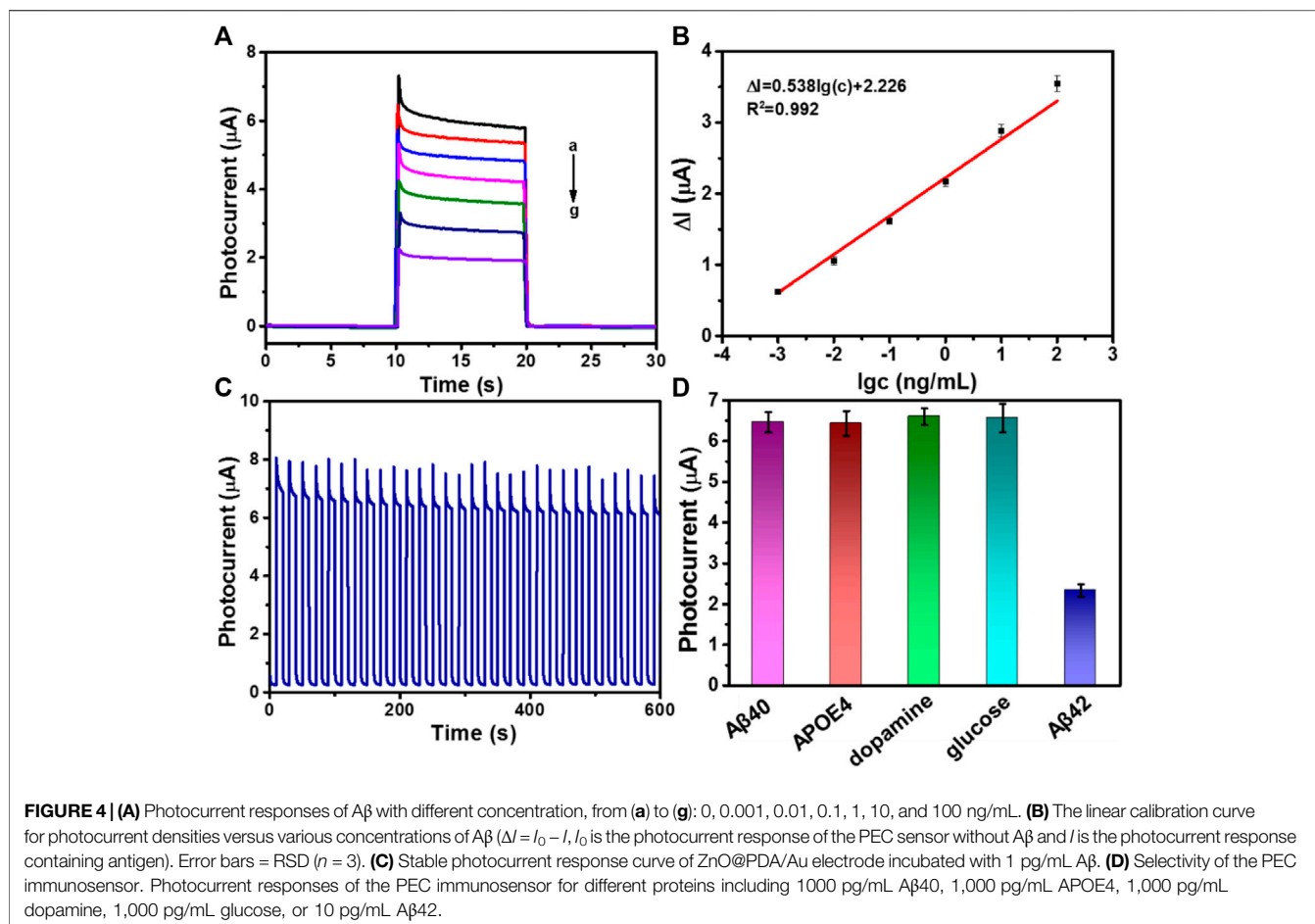
## RESULTS AND DISCUSSION

### Characterization of the as-prepared Electrodes

The morphology, structure, and composition of ZnO, ZnO@PDA, and ZnO@PDA/Au modified electrodes were recorded. The top and cross-sectional view SEM images in **Figure 2A**; **Supplementary Figure S1** display that a large scale of ZnO nanorods with lengths of around 1.2  $\mu\text{m}$  and diameters of less than 200 nm are grown on the ITO glass. The one-dimensional structure and large gap between the ZnO nanorods can provide a high surface area to facilitate light harvest and further biomaterial assembly. As shown in **Figure 2B**; **Supplementary Figure S2A**, after coating with PDA, the surface of modified nanorods become rougher compared with that of bare ZnO nanorods indicating that the ZnO nanorods have been successfully enwrapped by PDA to form a core/shell. The original structure of the ZnO nanorods still remained. The color of the substrate turns obviously from white to dark yellow during this process, as shown in **Supplementary Figure S3**. The ZnO@PDA were further used for *in situ* deposition of Au NPs basing on the reducing action of PDA coating. In **Figure 2C**; **Supplementary Figure S2B**, various Au NPs are observed homogeneously adhering on the surfaces of ZnO@PDA. At this time, the color

of the electrode turned dark red (**Supplementary Figure S3**). EDS spectrum was conducted to further analyze the elemental composition of the electrode with different modifications. The results in **Figure 1D** exhibit that the ZnO nanorods mainly contain Zn and O elements. The content of the C element increases after PDA coating providing another evidence for the existence of PDA. The distinctive Au signal of the ZnO@PDA/Au further confirms that Au has been introduced to the coating substrate successfully. **Figure 2E** shows the XRD patterns for the structural analysis of all the samples. The ZnO exhibits sharp diffraction peaks at 31.7°, 34.5°, 36.3°, 47.6°, and 62.9°, which could be assigned to the hexagonal ZnO phase (JCPDS No. 70–2551). Compared with the original ZnO, PDA-coated ZnO show no peak positions altering and additional peaks, indicating that wrapping PDA does not affect its crystal phase, while a minor increase of the peak intensity can be seen, which might be owing to the low content of PDA in the complex and the positive effect of PDA on the crystallization of ZnO. After loading Au NPs, the emerging characteristic peak of Au at 38.4° proves that Au NPs exist in the ZnO@PDA/Au composite.

Also, the optical properties of these samples were determined by UV–vis diffuse reflectance spectra (DRS). As presented in **Figure 2F**, the light absorbance of bare ZnO is weak in the visible region, which is ascribed to its intrinsic wide bandgap. However,



owing to the homogeneous coating of the PDA shell, ZnO@PDA shows an extended absorption range to the visible light region and increased absorption intensity, indicating that PDA can efficiently absorb visible light and works as a photosensitizer to improve the charge separation. The ZnO@PDA/Au exhibits an obvious absorption peak at about 560 nm, which is assigned to the SPR peak of Au NPs. The aforementioned results prove that by combining the PDA core-shell heterostructure and the LSPR effect of Au NPs, more photoelectric carriers can be generated and separated, which plays a crucial role in enhancing the utilization of sunlight for PEC sensing. In addition, the XPS spectrum is used to analyze the chemical composition and electronic structures of ZnO@PDA/Au. The XPS survey spectrum (Figure 2G) shows the existence of Zn, O, N, C, and Au elements in the hybrid composite. As displayed in Figure 2H, two peaks of Zn 2p at about 1,022.1 and 1,045.2 eV can be indexed to the binding energy of Zn 2p<sub>3/2</sub> and Zn 2p<sub>1/2</sub>, respectively. In Figure 2I, the O 1s peak is split into three peaks at 530.8, 531.5, and 532.3 eV, assigning to O-Zn bond binding energy in the structure of ZnO, O=C, and O-C in the PDA film, respectively (*Applied Surface Science* 457 (2018) 1096). As for the N 1s spectrum (Figure 3J), the three deconvoluted peaks centered at 398.4, 399.7, and 400.8 eV can be ascribed to primary (R = NH<sub>2</sub>), secondary (R-NH-R), and tertiary/aromatic

(=N-R) amine functional groups in PDA, respectively. The C 1s spectrum (Figure 3K) exhibits three characteristic peaks at 284.4 eV for CH<sub>x</sub> species, 285.1 eV for C-O/C-N, and 287.5 eV for C=O in PDA. In Figure 3L, the XPS spectrum of Au 4f strongly overlaps with the peaks of Zn 3p; thus, it was fitted into four peaks. The two peaks with the lower binding energy located in 83.1 and 86.8 eV have corresponded to the Au 4f<sub>7/2</sub> and Au 4f<sub>5/2</sub>, respectively. Meanwhile, another two peaks can be indexed to Zn 3p<sub>3/2</sub> (89.1 eV) and Zn 3p<sub>1/2</sub> (91.9 eV), respectively. Therefore, the aforementioned findings confirm the successful synthesis of ZnO@PDA/Au.

### Photoelectrochemical behaviors and charge transfer mechanism of the PEC immunosensor

Transient photocurrent, electrochemical impedance analysis (EIS), and linear sweep voltammograms (LSVs) were applied to estimate intrinsic electrochemical behavior and photocurrent response in the ZnO@PDA/Au system. The transient photocurrent responses of the as-fabricated electrodes have been measured at 0.05 V (Figure 3A). The ZnO@PDA/Au electrode owns the highest photocurrent, which is about fivefold of the pristine ZnO. The excellent PEC performance of ZnO@PDA/Au benefits from the synergistic action of PDA and

Au NPs, which broaden the light absorption range and enhance the separation efficiency of photo-generated electron-hole pairs. Moreover, EIS was used to test the electron transfer resistance change of different modification processes. As shown in **Figure 3B**, compared with ZnO and ZnO@PDA, the ZnO@PDA/Au shows the smallest interfacial electron transfer resistance.

The LSV curves of the ZnO, ZnO@PDA, and ZnO@PDA/Au electrodes were recorded in dark and under illumination with the applied potential ranging between  $-0.05$  and  $0.3$  V. As shown in **Figure 3C**, all the as-prepared photoelectrodes display negligible current in the dark condition although the current density of ZnO@PDA/Au is slightly higher than the other two electrodes. Under irradiation, the PDA-coated ZnO displays a higher photocurrent than that of the original ZnO. This increase of photocurrent is attributed to the enhanced light harvest capability by using PDA as the photosensitizer. Obviously, after the subsequent decoration of Au NPs on the ZnO@PDA, the photocurrent significantly increases under the same potential because of higher light absorption and the photocarriers' generation ability of Au nanoparticles. As a control, LSV curves of ITO are presented without/with simulated sunlight illumination, respectively, and the result is shown in **Supplementary Figure S4A**. Moreover, photocurrent responses of ITO, ITO/anti-A $\beta$ /BSA, and ITO/anti-A $\beta$ /BSA/A $\beta$  toward on/off cycles of simulated sunlight illumination at  $0.1$  V were also performed as shown in **Supplementary Figure S4B**. These results demonstrated that ITO has no PEC performance. According to the aforementioned analysis, the decoration of PDA and Au NPs on ZnO can bring excellent PEC performance.

According to the aforementioned results, the possible photo-generated charge transfer mechanism of the ZnO@PDA/Au is illustrated in **Figure 3D**. Under the solar light illumination, each component of the as-prepared photoanode could be excited to generate carriers simultaneously. Light irradiation of the ZnO induces the excited electrons from the valence band (VB) to the conduction band (CB) and further transfer to the surface of ITO. At the interface of PDA and ZnO, the generated electrons on the lowest unoccupied molecular orbital (LUMO) of PDA could transfer to the CB of ZnO to generate a built-in electric field due to the matching energy level, which effectively blocks the photo-generated charge recombination and enhance the charge separation and transfer efficiency. In addition, the plasmonic Au NPs could generate hot electrons with sufficient energy and inject into the LUMO of PDA under visible light excitation. The enriched electrons on the ZnO would transfer to the counter Pt photocathode through an external circuit to obtain the photocurrent signal for the PEC detection. Meanwhile, the remaining holes on the VB of ZnO transfer to the highest occupied molecular orbital of PDA. Both the accumulated holes on PDA and hot holes left on the Au NPs can be rapidly consumed by AA (electron donor) in the electrolyte against the photoinduced carrier recombination. Accordingly, by integrating the photosensitization of PDA and LSPR effect of Au NPs, the ZnO@PDA/Au is considered to be an excellent substrate material for photocurrent response.

## Optimization of Detection Conditions

To obtain the best detection performance of photoelectrode, the AA concentration and the pH values, which have a direct effect on PEC response signal through electron transfer, were optimized in detail. AA can be used as the scavenger to consume the photoinduced hole and an efficient antioxidant to reduce the photo-oxidized PDA film. The change of photocurrent with the AA concentration range from  $0.01$  to  $100$  mM is shown in **Supplementary Figure S5A**. The photocurrent signal of the ZnO@PDA/Au electrode displays a significant increment along with the increasing AA concentration at first and then reaches a peak at  $1$  mM. A decrease in photocurrent density can be seen, when the AA concentration in the solution continues to increase. When the photo-generated electrons are injected into ZnO, the PDA and Au NPs could be regenerated through gaining electrons from the electron donor to achieve effective separation of photo-generated charge. At the same time, the excess AA in the electrolyte solution leads to the quenching absorption of the solution, which impacts the irradiation reaching the photoanode and reduces the intensity and efficiency of the excitation electron-hole center. Thus,  $1$  mM was selected as the optimal concentration of AA in this work.

Furthermore, the effect of pH value on the detection photocurrent was recorded in **Supplementary Figure S5B**. The photocurrent gradually increases with the pH of the buffer solution rising from  $6.5$  to  $7.4$ . When the pH value further enhances to  $8.5$ , the photocurrent shows an obvious decrement. This result may be ascribed to the bioactivity of the immobilized antigen that could be disrupted in the acidic or alkaline environment. The PBS solution with pH  $7.4$  is similar to the physiological environment to maintain the good activity of the biomolecules. Thus, to obtain an excellent photocurrent response and immunocomplex layer on the photoanode, pH  $7.4$  was selected in the following detection. In addition, the concentration of antibody was optimized, and the result shows the optimal concentration is  $10$   $\mu$ g/mL (**Supplementary Figure S6**).

## Analytical Performance of the Photoelectrochemical Immunosensor

Based on the aforementioned optimal conditions, the photocurrent density was collected to track the succession process for the fabrication of the PEC immunosensor. In **Supplementary Figure S7**, after the immobilization of anti-A $\beta$  (curve b) and subsequent BSA blocking (curve c), the photocurrent intensity reduces significantly. This is ascribed to the binding molecules on the surface of the photoanode that partly hinder the access and reaction of AA with the photoinduced holes. The further decrease of photocurrent can be seen after continued incubation with A $\beta$ , owing to the formation of the antigen-antibody immunocomplexes on the photoelectrode surface. These results confirm the successful construction of the label-free PEC immunosensor.

The photocurrent intensity has a direct relationship with the concentration of A $\beta$ . Thus, the as-fabricated immunosensor based on ZnO@PDA/Au was applied to detect A $\beta$  with different concentrations. **Figure 4A** displays the photocurrent change of the as-fabricated PEC biosensor with different concentrations of A $\beta$  at the optimal condition. It can be seen that along with the

increase of the A $\beta$  concentration, the photocurrent reduces gradually. The linear relationship related to the change of the photocurrent intensity ( $\Delta I$ ) and the logarithm of A $\beta$  concentration in the range from 1 pg mL<sup>-1</sup> to 100 ng mL<sup>-1</sup> is presented in **Figure 4B**. The regression equation is displayed as  $\Delta I = 0.538 \log c + 2.226$  ( $R^2 = 0.992$ ). The limit of detection (LOD) is determined to be 0.26 pg mL<sup>-1</sup> (S/N = 3). The LOD is calculated by three times the SD of the blank according to our previous report. (Yibiao, Qing et al., 2021) As a control, a typical ELISA has been used to validate our method. As shown in **Supplementary Figure S8**, the ELISA calibration curve was constructed by plotting the optical density of A $\beta$ 42 at 450 nm (TMB as substrate). And the range of A $\beta$ 42 concentration is 1–800 pg/mL. The relationship between the optical density at 450 nm and the A $\beta$ 42 concentration follows the regression equation  $y = 0.00099x + 0.072$  ( $R^2 = 0.9991$ ). The detection limit is 18.59 pg/mL, and the linear range is from 10 to 800 pg/mL. Compared with typical ELISA, our prepared PEC sensor based on ZnO@PDA/Au exhibited lower LOD and wider linear range. Compared with several previous reports for the detection of A $\beta$ , the proposed PEC immunosensor in our work exhibits a much wider sensing range and competitive LOD. A comparison is shown in Supplementary Table S1. What is more, the as-fabricated material is environment friendly and possesses good biocompatibility. Therefore, the ZnO@PDA/Au is a very promising material used for the construction of sensitive PEC immunosensors.

### Stability, Reproducibility, and Specificity

The stability, reproducibility, and specificity are very crucial factors for the successful construction of immunosensor in biological application. The photocurrent response of as-prepared immunosensor incubated with 1 pg mL<sup>-1</sup> A $\beta$  was tested by 30 on/off cycles of illumination to access its stability. Observing from **Figure 4C**, the photocurrent response shows no distinct variation. Moreover, the as-fabricated immunosensor was stored at 4°C to investigate the storage stability. After 2 weeks of restoring, the photocurrent density could still retain 90.1% of its initial response (**Supplementary Figure S9**). In addition, the reproducibility of this ZnO@PDA/Au electrode was also measured, and the result is shown in **Supplementary Figure S10**, which demonstrated that the ZnO@PDA/Au electrode had excellent reproducibility. To evaluate the specificity of the fabricated PEC biosensor, several biological interfering species including A $\beta$ 40, human apolipoprotein E4 (APOE4), dopamine, and glucose with a 100-fold higher concentration were chosen for the test. As shown in **Figure 4D**, the photocurrent response to the interfering substances appears imperceptible, compared with that of the specific target A $\beta$ 42, which implied that the PEC immunosensor possesses excellent anti-interference ability and specificity. The aforementioned results prove that this proposed sensing platform owns superior stability, reproducibility, and specificity.

### A $\beta$ Detection in Serum Sample

To further certify the practicability of the prepared PEC immunosensor, the tests were also carried out in real biological samples. The diluted serum samples were spiked with different concentrations of A $\beta$ 42 (1, 10, 100, 1,000, 10,000 pg/mL), and then the photocurrent changes were recorded in Supplementary Table S2. The detection results are close to that of the added values with satisfactory recoveries ranging from 97.1 to 109.1%, revealing that

the proposed PEC immunosensor based on ZnO@PDA/Au has excellent sensitivity and reliability for the detection of A $\beta$  in real serum sample analysis and can be capable for the clinical diagnosis.

## CONCLUSION

In summary, a novel PEC immunosensor based on PDA and Au NP co-decorated ZnO was successfully designed for ultrasensitive and label-free detection of A $\beta$ . The ZnO@PDA/Au substrate obtained by self-polymerization and *in situ* self-reduction exhibits superior optoelectronic property by taking the advantage of the photosensitization of PDA and SPR effect of Au NPs together. What is more, the PDA film and Au NPs can also be used as a biocompatible functional layer for the immobilization of biomolecules. The interfacial charge transfer mechanism of the proposed biosensing platform was investigated in detail. The as-fabricated PEC immunosensor displays apparent merits for A $\beta$  detection including broad linear range, low detection limit, and good anti-interference performance and stability. In addition, it can also realize the acceptable quantitative analysis of A $\beta$  in real serum sample. Due to the aforementioned advantages, the PEC electrode provides a versatile sensing platform and has good potential in other bioanalysis applications for early disease diagnosis.

## DATA AVAILABILITY STATEMENT

The original contributions presented in the study are included in the article/**Supplementary Material**, further inquiries can be directed to the corresponding authors.

## AUTHOR CONTRIBUTIONS

YL elaborated the concept and revised the article. Baochengyang and SZ supervised the paper. GH, YZ, ML, YG, and HY consulted literature, reorganized materials and drew the figures. All the authors participated in scientific discussions and wrote the paper.

## FUNDING

This work was supported by the Natural Science Foundation of China (51872110), Guangdong-Hong Kong-Macao Greater Bay Area Center for Brain Science and Brain-Inspired Intelligence Fund (NO.2019027), the Training Program of Youth Backbone Teacher of Henan Province of 2018 (2018GGJS178), the special fund project of Zhengzhou basic and applied basic research (ZZSZX202001 and ZZSZX202002).

## SUPPLEMENTARY MATERIAL

The Supplementary Material for this article can be found online at: <https://www.frontiersin.org/articles/10.3389/fbioe.2021.777344/full#supplementary-material>

## REFERENCES

- Brazaca, L. C., Sampaio, I., Zucolotto, V., and Janegitz, B. C. (2020). Applications of Biosensors in Alzheimer's Disease Diagnosis. *Talanta* 210, 120644. doi:10.1016/j.talanta.2019.120644
- Butterfield, D. A., Drake, J., Pocernich, C., and Castegna, A. (2002). Evidence of Oxidative Damage in Alzheimer's Disease Brain: central Role for Amyloid Beta-Peptide. *Trends Mol. Med.* 7, 548–554. doi:10.1016/S1471-4914(01)02173-6
- Carneiro, P., Loureiro, J., Delerue-Matos, C., Morais, S., and do Carmo Pereira, M. (2017). Alzheimer's Disease: Development of a Sensitive Label-free Electrochemical Immunosensor for Detection of Amyloid Beta Peptide. *Sensors Actuators B: Chem.* 239, 157–165. doi:10.1016/j.snb.2016.07.181
- Dong, X., Xu, C., Yang, C., Chen, F., Manohari, A. G., Zhu, Z., et al. (2019). Photoelectrochemical Response to Glutathione in Au-Decorated ZnO Nanorod Array. *J. Mater. Chem. C* 7, 5624–5629. doi:10.1039/c9tc00901a
- Evans, D. A., Funkenstein, H. H., Albert, M. S., Scherr, P. A., Cook, N. R., and Chown, M. J. (1989). Prevalence of Alzheimer's Disease in a Community Population of Older Persons. *Jama* 262, 2551–2556. doi:10.1001/jama.1989.03430180093036
- Fang, W.-K., Liu, L., Zhang, L.-L., Liu, D., Liu, Y., and Tang, H.-W. (2021). Detection of Amyloid  $\beta$  Oligomers by a Fluorescence Ratio Strategy Based on Optically Trapped Highly Doped Upconversion Nanoparticles-SiO<sub>2</sub>@Metal-Organic Framework Microspheres. *Anal. Chem.* 93, 12447–12455. doi:10.1021/acs.analchem.1c02679
- Folego, G., Weiler, M., Casseb, R. F., Pires, R., and Rocha, A. (2020). Alzheimer's Disease Detection through Whole-Brain 3D-CNN MRI. *Front. Bioeng. Biotechnol.* 8. doi:10.3389/fbioe.2020.534592
- Gasparotto, G., Costa, J. P. C., Costa, P. I., Zaghete, M. A., and Mazon, T. (2017). Electrochemical Immunosensor Based on ZnO Nanorods-Au Nanoparticles Nanohybrids for Ovarian Cancer Antigen CA-125 Detection. *Mater. Sci. Eng. C* 76, 1240–1247. doi:10.1016/j.msec.2017.02.031
- Grimmer, T., Riemenschneider, M., Förstl, H., Henriksen, G., Klunk, W. E., Mathis, C. A., et al. (2009). Beta Amyloid in Alzheimer's Disease: Increased Deposition in Brain Is Reflected in Reduced Concentration in Cerebrospinal Fluid. *Biol. Psychiatry* 65, 927–934. doi:10.1016/j.biopsych.2009.01.027
- Hardy, J., and Selkoe, D. J. (2002). The Amyloid Hypothesis of Alzheimer's Disease: Progress and Problems on the Road to Therapeutics. *Science* 297, 353–356. doi:10.1126/science.1072994
- He, G., Gao, F., Li, W., Li, P., Zhang, X., Yin, H., et al. (2019). Electrochemical Sensing of H<sub>2</sub>O<sub>2</sub> Released from Living Cells Based on AuPd alloy-modified PDA Nanotubes. *Anal. Methods* 11, 1651–1656. doi:10.1039/C8AY02743A
- Hu, W., He, G., Zhang, H., Wu, X., Li, J., Zhao, Z., et al. (2014). Polydopamine-Functionalization of Graphene Oxide to Enable Dual Signal Amplification for Sensitive Surface Plasmon Resonance Imaging Detection of Biomarker. *Anal. Chem.* 86, 4488–4493. doi:10.1021/ac5003905
- Jack, C. R., Knopman, D. S., Jagust, W. J., Shaw, L. M., Aisen, P. S., Weiner, M. W., et al. (2010). Hypothetical Model of Dynamic Biomarkers of the Alzheimer's Pathological cascade. *Lancet Neurol.* 9, 4–5. doi:10.1016/S1474-4422(09)70299-6
- Kang, Z., Yan, X., Wang, Y., Zhao, Y., Bai, Z., Liu, Y., et al. (2016). Self-powered Photoelectrochemical Biosensing Platform Based on Au NPs@ZnO Nanorods Array. *Nano Res.* 9, 344–352. doi:10.1007/s12274-015-0913-9
- Lee, H., Dellatore, S. M., Miller, W. M., and Messersmith, P. B. (2007). Mussel-Inspired Surface Chemistry for Multifunctional Coatings. *Science* 318, 426–430. doi:10.1126/science.1147241
- Lee, S.-C., Park, H.-H., Kim, S.-H., Koh, S.-H., Han, S.-H., and Yoon, M.-Y. (2019). Ultrasensitive Fluorescence Detection of Alzheimer's Disease Based on Polyvalent Directed Peptide Polymer Coupled to a Nanoporous ZnO Nanoplatfrom. *Anal. Chem.* 91, 5573–5581. doi:10.1021/acs.analchem.8b03735
- Liu, Y., Ai, K., and Lu, L. (2014). Polydopamine and its Derivative Materials: Synthesis and Promising Applications in Energy, Environmental, and Biomedical Fields. *Chem. Rev.* 114, 5057–5115. doi:10.1021/cr400407a
- Liu, Y., Xu, Q., Zhang, Y., Ren, B., Huang, L., Cai, H., et al. (2021). An Electrochemical Aptasensor Based on AuPt alloy Nanoparticles for Ultrasensitive Detection of Amyloid- $\beta$  Oligomers. *Talanta* 231, 122360. doi:10.1016/j.talanta.2021.122360
- Lynge, M. E., van der Westen, R., Postma, A., and Städler, B. (2011). Polydopamine-a Nature-Inspired Polymer Coating for Biomedical Science. *Nanoscale* 3, 4916–4928. doi:10.1039/C1NR10969C
- Marcus, C., Mena, E., and Subramaniam, R. M. (2014). Brain PET in the Diagnosis of Alzheimer's Disease. *Clin. Nucl. Med.* 39, e413–6. doi:10.1097/RLU.0000000000000547
- Matthews, F. E., Arthur, A., Barnes, L. E., Bond, J., Jagger, C., Robinson, L., et al. (2013). A Two-Decade Comparison of Prevalence of Dementia in Individuals Aged 65 Years and Older from Three Geographical Areas of England: Results of the Cognitive Function and Ageing Study I and II. *The Lancet* 382, 1405–1412. doi:10.1016/S0140-6736(13)61570-6
- Murphy, M. P., and LeVine, H. (2010). Alzheimer's Disease and the Amyloid- $\beta$  Peptide. *Jad* 19, 311–323. doi:10.3233/jad-2010-1221
- Nakamura, A., Kaneko, N., Villemagne, V. L., Kato, T., Doecke, J., Doré, V., et al. (2018). High Performance Plasma Amyloid- $\beta$  Biomarkers for Alzheimer's Disease. *Nature* 554, 249–254. doi:10.1038/nature25456
- Norouzi, P., Gupta, V. K., Faridbod, F., Pirali-Hamedani, M., Larijani, B., and Ganjali, M. R. (2011). Carcinoembryonic Antigen Admittance Biosensor Based on Au and ZnO Nanoparticles Using FFT Admittance Voltammetry. *Anal. Chem.* 83, 1564–1570. doi:10.1021/ac102270w
- Obata, Y., Murakami, K., Kawase, T., Hirose, K., Izuo, N., Shimizu, T., et al. (2020). Detection of Amyloid  $\beta$  Oligomers with RNA Aptamers in AppNL-G-F/NL-G-F Mice: A Model of Arctic Alzheimer's Disease. *ACS Omega* 5, 21531–21537. doi:10.1021/acsomega.0c02134
- Selkoe, D. J. (2012). Preventing Alzheimer's Disease. *Science* 337, 1488–1492. doi:10.1126/science.1228541
- Shu, J., and Tang, D. (2019). Recent Advances in Photoelectrochemical Sensing: From Engineered Photoactive Materials to Sensing Devices and Detection Modes. *Anal. Chem.* 92, 363–377. doi:10.1021/acs.analchem.9b04199
- Song, L., Lachno, D. R., Hanlon, D., Shepro, A., Jeromin, A., Gemani, D., et al. (2016). A Digital Enzyme-Linked Immunosorbent Assay for Ultrasensitive Measurement of Amyloid- $\beta$  1-42 Peptide in Human Plasma with Utility for Studies of Alzheimer's Disease Therapeutics. *Alz Res. Ther.* 8, 58–64. doi:10.1186/s13195-016-0225-7
- Wang, R., Ma, H., Zhang, Y., Wang, Q., Yang, Z., Du, B., et al. (2017). Photoelectrochemical Sensitive Detection of Insulin Based on CdS/polydopamine Co-sensitized WO<sub>3</sub> Nanorod and Signal Amplification of Carbon Nanotubes@polydopamine. *Biosens. Bioelectron.* 96, 345–350. doi:10.1016/j.bios.2017.05.029
- Wang, X. Z., Du, J., Xiao, N. N., Zhang, Y., Fei, L., LaCoste, J. D., et al. (2020). Driving Force to Detect Alzheimer's Disease Biomarkers: Application of a Thioflavine T@Er-MOF Ratiometric Fluorescent Sensor for Smart Detection of Presenilin 1, Amyloid  $\beta$ -protein and Acetylcholine. *Analyst* 145, 4646–4663. doi:10.1039/D0AN00440E
- Wang, Y., Fan, D., Zhao, G., Feng, J., Wei, D., Zhang, N., et al. (2018). Ultrasensitive Photoelectrochemical Immunosensor for the Detection of Amyloid  $\beta$ -protein Based on SnO<sub>2</sub>/SnS<sub>2</sub>/Ag<sub>2</sub>S Nanocomposites. *Biosens. Bioelectron.* 120, 1–7. doi:10.1016/j.bios.2018.08.026
- Wei, Y., Ke, L., Kong, J., Liu, H., Jiao, Z., Lu, X., et al. (2012). Enhanced Photoelectrochemical Water-Splitting Effect with a Bent ZnO Nanorod Photoanode Decorated with Ag Nanoparticles. *Nanotechnology* 23, 235401. doi:10.1088/0957-4484/23/23/235401
- Xiao, S., Liu, P., Zhu, W., Li, G., Zhang, D., and Li, H. (2015). Copper Nanowires: A Substitute for Noble Metals to Enhance Photocatalytic H<sub>2</sub> Generation. *Nano Lett.* 15, 4853–4858. doi:10.1021/acs.nanolett.5b00082
- Yang, J. K., Hwang, I. J., Cha, M. G., Kim, H. I., Yim, D., Jeong, D. H., et al. (2019). Reaction Kinetics-Mediated Control over Silver Nanogap Shells as Surface-Enhanced Raman Scattering Nanoprobes for Detection of Alzheimer's Disease Biomarkers. *Small* 15, 1900613. doi:10.1002/sml.201900613
- Yang, X., Li, H., Zhang, W., Sun, M., Li, L., Xu, N., et al. (2017). High Visible Photoelectrochemical Activity of Ag Nanoparticle-Sandwiched CdS/Ag/ZnO Nanorods. *ACS Appl. Mater. Inter.* 9, 658–667. doi:10.1021/acsami.6b12259
- Yang, Y., and Hu, W. (2017). Bifunctional Polydopamine Thin Film Coated Zinc Oxide Nanorods for Label-free Photoelectrochemical Immunoassay. *Talanta* 166, 141–147. doi:10.1016/j.talanta.2017.01.024
- Yang, Z., Wang, Y., and Zhang, D. (2021). 2021 Alzheimer's Disease Facts and Figures. *Alzheimer's Dement.* 17, 327–406. doi:10.1002/alz.12328

- Yu, Y., Huang, Z., Zhou, Y., Zhang, L., Liu, A., Chen, W., et al. (2019). Facile and Highly Sensitive Photoelectrochemical Biosensing Platform Based on Hierarchical Architected Polydopamine/Tungsten Oxide Nanocomposite Film. *Biosens. Bioelectron.* 126, 1–6. doi:10.1016/j.bios.2018.10.026
- Zhang, B., Wang, F., Zhu, C., Li, Q., Song, J., Zheng, M., et al. (2016). A Facile Self-Assembly Synthesis of Hexagonal ZnO Nanosheet Films and Their Photoelectrochemical Properties. *Nano-micro Lett.* 8, 137–142. doi:10.1007/s40820-015-0068-y
- Zhang, B., Wang, H., Ye, H., Xu, B., Zhao, F., and Zeng, B. (2018). Reversible Redox Mechanism Based Synthesis of Plasmonic WO<sub>3</sub>/Au Photocatalyst for Selective and Sensitive Detection of Ultra-micro Hg<sup>2+</sup>. *Sensors Actuators B: Chem.* 273, 1435–1441. doi:10.1016/j.snb.2018.07.070
- Zhang, Y., He, S., Guo, W., Hu, Y., Huang, J., Mulcahy, J. R., et al. (2018). Surface-Plasmon-Driven Hot Electron Photochemistry. *Chem. Rev.* 118, 2927–2954. doi:10.1021/acs.chemrev.7b00430
- Zheng, Y., Zheng, L., Zhan, Y., Lin, X., Zheng, Q., and Wei, K. (2007). Ag/ZnO Heterostructure Nanocrystals: Synthesis, Characterization, and Photocatalysis. *Inorg. Chem.* 46, 6980–6986. doi:10.1021/ic700688f
- Zhou, X., Wang, S., Zhang, C., Lin, Y., Lv, J., Hu, S., et al. (2021). Colorimetric Determination of Amyloid- $\beta$  Peptide Using MOF-Derived Nanozyme Based on Porous ZnO-Co<sub>3</sub>O<sub>4</sub> Nanocages. *Microchim Acta* 188, 56. doi:10.1007/s00604-021-04705-4
- Zhu, Y.-C., Zhang, N., Ruan, Y.-F., Zhao, W.-W., Xu, J.-J., and Chen, H.-Y. (2016). Alkaline Phosphatase Tagged Antibodies on Gold Nanoparticles/TiO<sub>2</sub> Nanotubes Electrode: A Plasmonic Strategy for Label-free and Amplified Photoelectrochemical Immunoassay. *Anal. Chem.* 88, 5626–5630. doi:10.1021/acs.analchem.6b01261

**Conflict of Interest:** The authors declare that the research was conducted in the absence of any commercial or financial relationships that could be construed as a potential conflict of interest.

**Publisher's Note:** All claims expressed in this article are solely those of the authors and do not necessarily represent those of their affiliated organizations, or those of the publisher, the editors, and the reviewers. Any product that may be evaluated in this article, or claim that may be made by its manufacturer, is not guaranteed or endorsed by the publisher.

Copyright © 2021 He, Zhou, Li, Guo, Yin, Yang, Zhang and Liu. This is an open-access article distributed under the terms of the Creative Commons Attribution License (CC BY). The use, distribution or reproduction in other forums is permitted, provided the original author(s) and the copyright owner(s) are credited and that the original publication in this journal is cited, in accordance with accepted academic practice. No use, distribution or reproduction is permitted which does not comply with these terms.